Centrifuge modelling of monotonic and cyclic lateral responses of monopiles in quartz and carbonate sands

Márcio de Sousa Soares de Almeida[1], *Maria Fernanda Wamser Barra*[2], *Naiala Fidelis Gomes*[3], *José Wedney Pereira Gomes*[4], *Maria Cascão Ferreira de Almeida*[5], *Marcos Massao Futai*[6]

[1, 2, 3, 4] *Graduate School of Engineering, Federal University of Rio de Janeiro, Rio de Janeiro, Brazil*
[5] *Polytechnic School, Federal University of Rio de Janeiro, Rio de Janeiro*
[6] *Department of Structural and Geotechnical Engineering, University of Sao Paulo, São Paulo*
[#] *Corresponding author: wedney.ecivil@gmail.com*

ABSTRACT

This study evaluates the soil-structure interaction of monopiles subjected to monotonic and cyclic lateral loading by means of centrifuge modelling. The monopile were installed in two types of dense sands: quarts and carbonate. To evaluate the static and dynamic properties, the two soils were characterized by index tests, as well as triaxial, resonant column and bender element tests. The triaxial tests showed that angles of internal friction were higher for the sand with higher carbonate content ($CaCO_3$). Also, curved shear strength envelopes were observed in both soils, i.e., peak friction angles decreasing with confining stress. Regarding the dynamic soil properties, the stress history appears to affect the stiffness of the carbonate sands more than the quartz sands, i.e., the higher $CaCO_3$ content soil exhibited greater shear modulus degradation. In the geotechnical centrifuge tests the lateral loading capacity about doubled after 4800 loading cycles, slightly more for the carbonate sand than for the quartz sand. Also, as a function of the cycling process, the secant stiffness increased for both sand types, especially in the first 500 loading cycles where the increase occurred exponentially.

Keywords: centrifuge modeling; monopile; carbonate sand; offshore wind turbine.

1. Introduction

Over the last few years there has been significant growth in the offshore wind energy industry, especially in European and Asian countries. The latest annual report from the Global Wind Energy Council (GWEC 2022), reported that 2021 was a record year for offshore wind power, with a total of 21.1 gigawatts (GW) of new capacity brought online. Brazil alone has enormous potential for the offshore wind energy sector. There are 36 projects in the licensing phase in Brazil with a total planned capacity of 80 GW (EPBR, 2022).

In the shallow water region of most of the Brazilian coastline, there is a significant presence of calcium carbonate $CaCO_3$ (OECO, 2021). Carbonate sands are fragile, with particles generally more crushable and compressible than quartz sands, therefore demanding special attention for the installation of foundations in these soil types (El-Reedy, 2020). Studies on the soil-structure interaction of soils with the presence of $CaCO_3$ are scarce (e.g., Dyson and Randolph, 2001), especially in the context of the interaction with offshore wind turbine foundations.

About 75% of installed offshore wind turbine foundations (OWM, 2021) are monopile foundations. Monopiles have a length L to diameter D ratio in the order of 5, whereas conventional pile foundations typically have an L/D ratio on the order of 20. Additionally, offshore wind turbines are subjected to cyclical environmental and operational loads, which impose repetitive loads on the structure and foundation. This overall scenario has prompted numerous studies on monopile foundations worldwide (e.g., Buckley et al., 2020; Byrne et al., 2020).

The study presented here uses centrifuge modelling to evaluate the soil-structure interaction of monopiles installed in two types of dense sands: quartz and carbonate. The monopiles were subjected to monotonic and cyclic lateral loads aiming to evaluate two important design conditions. On the one hand, the Serviceability Limit State (SLS), in this case, is evaluated through the change in secant stiffness and accumulation of displacement as a function of the number of loading cycles, and on the other hand, the Ultimate Limit State (ULS), i.e., the lateral load capacity. Centrifuge modeling of monopiles has been used frequently for advancing the understanding of monopile behavior in quartz sand (e.g., Abadie et al., 2019; Futai et al., 2018). Fig. 1 shows a wind tower with a monopile foundation, illustrating the lateral loading scheme generally used in physical modeling. As a background for the interpretation of the results of the centrifuge tests, the static and dynamic properties of the two soils tested are presented initially.

2. Behavior of the quartz and carbonate sands used in the centrifuge tests

Natural carbonate sands have complex characteristics, including high intraparticle porosity that make them unsuitable for use in centrifuge modeling (Watson et. al., 2019). A first requirement of the sandy soil used in centrifuge modeling is uniform grain size to enable model preparation. A second requirement is to have a pile diameter (D) to average grain size (d_{50}) ratio greater than 88 (Klinkvort, 2012), in order to overcome

the scale effect with respect to the grains, a requirement generally not met by natural carbonate sands. Given these limitations, artificial carbonate sands were used as an alternative in the centrifuge tests. It is important to recognize, however, that differences exist between natural and artificial carbonate sands because sediments are subject to various forms of degradation in the marine environment with respect to mass transport processes (Watson et. al., 2019).

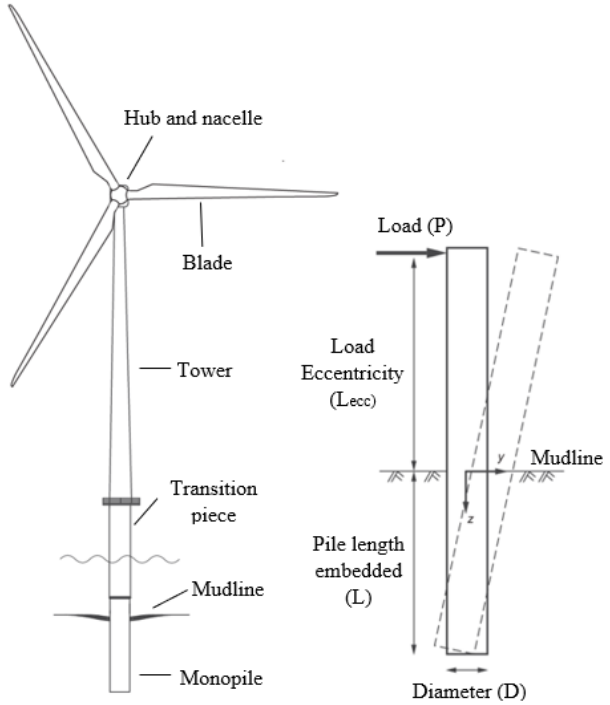

Figure 1. Offshore wind tower with monopile foundation.

2.1. Index and Physico-chemical tests

Index and physico-chemical tests were performed on quartz sand (QZ) and artificial carbonate sand with 80% $CaCO_3$ by weight (CA80). Fig. 2 shows two Scanning Electron Microscope (SEM) images for the carbonate and quartz sands. It can be observed that the CA80 sand has more irregular particles than the QZ sand. The presence of porous grains is also visible in the CA80 sand.

Table 1 summarizes the results obtained in the physico-chemical tests, which include the percentage of $CaCO_3$, specific gravity of soil grains (G_s), maximum (e_{max}) and minimum (e_{min}) void ratio, and average grain diameter (d_{50}). All sands were classified as uniform and well graded. The results presented in Table 1 are consistent with the literature (e.g., Poulos, 1982; Almeida et al., 1987) and are in agreement with offshore test results on carbonate sand from the Northeast region of Brazil (Garske, 2020).

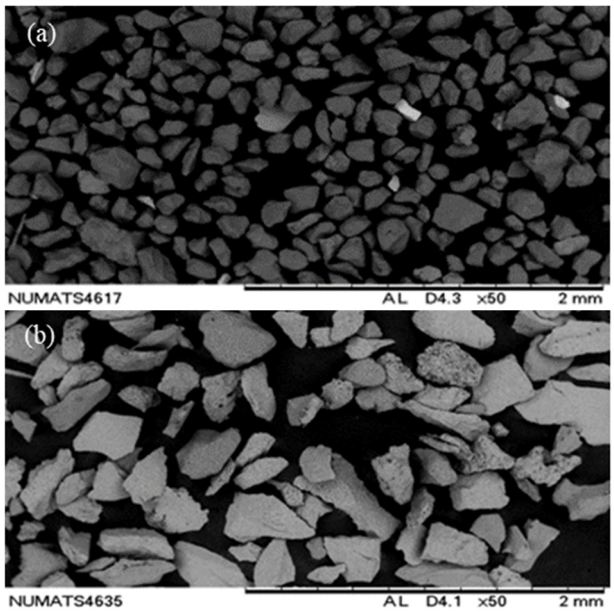

Figure 2. SEM images of the QZ sand (a) and the CA80 sand (b).

Table 1. The main characteristics of the QZ and CA80 sands

Sand	$CaCO_3$ (%)	G_s	e_{max}	e_{min}	d_{50} (mm)	γ_n (1) (kN/m^3)
QZ	0.0 - 0.4	2.638	0.915	0.602	0.18	15.5
CA80	80.2 - 81.4	2.817	1.247	0.862	0.18	14.3
Offshore NE Brazil(2)	35.7 - 80	-	0.804 - 1.464	0.567 - 0.795	-	-

(1) Unit weight for Relative Density (Dr) equal to 80% (reference value used in the centrifuge tests).
(2) Personal communication (Ricardo Garske, 2020).

2.2. Shear Strength

Consolidated drained (CD) triaxial tests were performed on specimens (50 mm x 100 mm) subjected to confining stress between 50 kPa and 600 kPa. The specimens were prepared using the dry pluviation technique (Miura and Toki, 1982) for nominal values of Relative Density D_r equal to 80% and test results are presented in Fig. 3.

The deviatoric stress-axial strain plot in Fig. 3 (a), indicates a higher shear strength for the CA80 sand than the QZ sand. This result seems to be due to the more angular grains of the CA80 sand, as illustrated in Fig. 2.

The volumetric strain versus axial strain results, Fig. 3 (b), show that the CA80 sand tends to dilate less than QZ sand. According to Almeida et al. (1987) carbonate sands tend to dilate less than quartz sands due to the tendency for crushing and breakage of the grains. Grain size analyses after triaxial tests indicated an approximately constant percentage of fines (% passing sieve #200), 1% to 2%, for the QZ sand for the range of confining stresses adopted, 50 kPa to 600 kPa. However, for the CA80 sand, the fines increased with the confining stresses from 1% to 5%.

Finally, the results show an increase in the peak friction angle with the percentage of $CaCO_3$, as can be seen in Fig. 3 (c). Tests performed on carbonate sands with 50% $CaCO_3$ by weight (CA50) showed intermediate

results between the QZ and CA80 sands, not presented here due to space limitations.

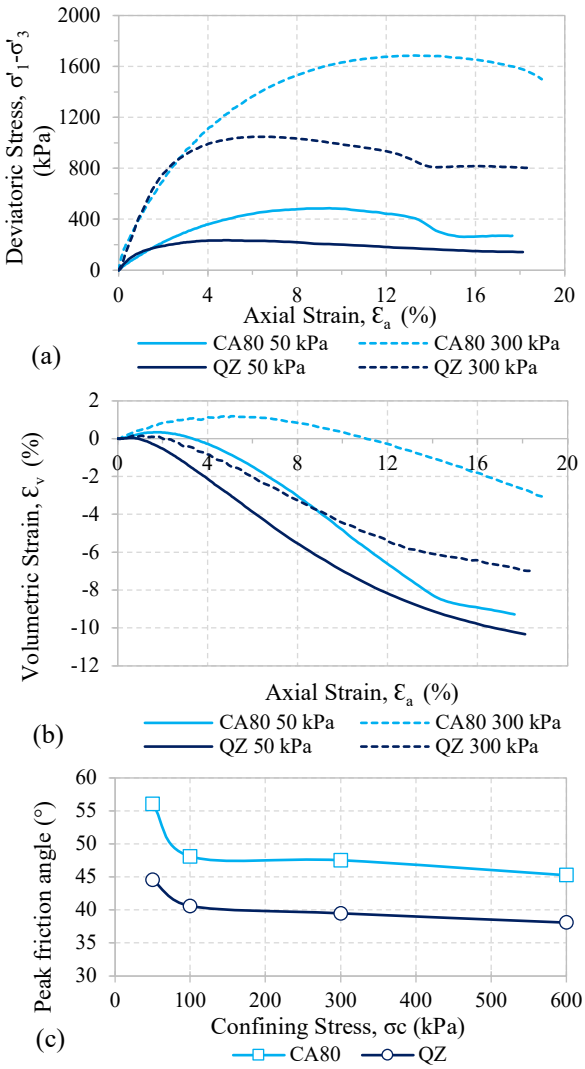

Figure 3. Results of the triaxial tests.

2.3. Shear modulus and damping

Resonant column tests were performed in order to obtain the shear modulus (G) and damping (D) for small values of shear strains (γ), for the same range of confining stress adopted in the triaxial tests presented previously. The test performed was of the fixed-base free top type with a rigid mass on top (Drnevich et al., 2015). Further details of the equipment and applications can be seen in Correia et al. (2001). Specimens with a 35 mm diameter and 80 mm height were prepared with the dry pluviation technique for the relative density Dr equal to 80%. The resonant column tests, performed according to the recommendations of the ASTM D4015 (2017), consisted of applying increasing confining stress between 50 kPa and 600 kPa, and with measurements of G, D, and γ for each confining stress value. Next, measurements were performed for decreasing confining stress.

Measurements of the small strain shear modulus G_{max} obtained by resonant column tests, for increasing and decreasing stresses, are presented in Fig. 4. The result for the QZ sand shows little difference in the G_{max} values at loading and unloading. However, for the CA80 sand, the values of G_{max} at unloading are higher than at loading. This behavior is attributable to the visco-plastic to brittle nature of the contact response of carbonate soil particles (Senetakis and Madhusudhan 2015). In other words, the stress history appears to affect the stiffness of carbonate sands more than quartz sands. The G_{max} measurements for the QZ sand agreed well with the equation proposed by Menq (2003). G_{max} measurements carried out with bender element tests showed a similar pattern to Resonant Column test results.

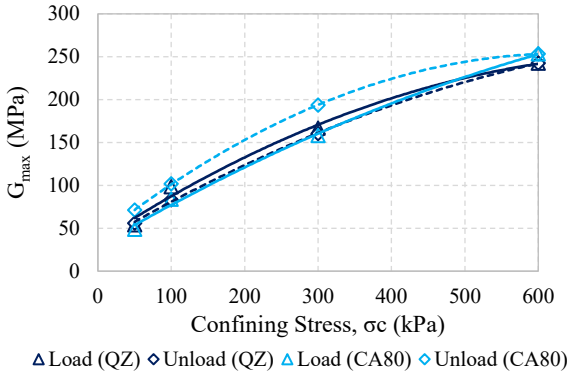

Figure 4. G_{max} as a function of confining stress.

Fig. 5 shows the results of the resonant column tests with normalized values of G (by G_{max} measurements) and D. The experimental results for the QZ sand compare well with the models of Menq (2003). With respect to the CA80 sand, the best fit model was that of Flores Lopez et al., (2018) which takes into account the influence of the percentage of $CaCO_3$. Note that, for any value of shear strain the carbonate sand presents lower shear modulus in comparison with the quartz sand.

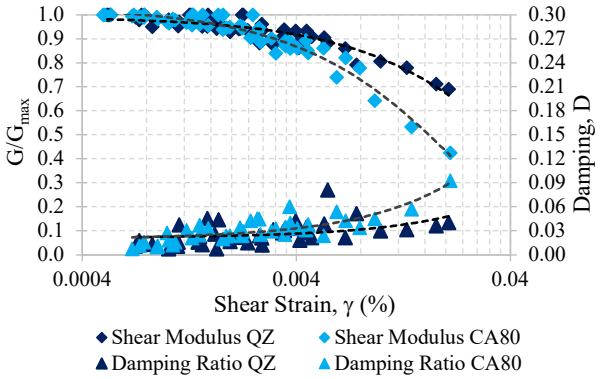

Figure 5. Values of G and D as a function of γ.

3. Physical modeling of a monopile in a geotechnical centrifuge

3.1. Materials and methods

The soil-structure interaction tests were performed on the 9 g-ton arm geotechnical centrifuge of the Multiuser Laboratory in Centrifuge Modeling (LM2C) of the Federal University of Rio de Janeiro (UFRJ), whose detailed description can be found in Almeida et. al. (2014). Particular mention is made for the servomotor-controlled bidirectional actuator used in the present study. The principles of physical modeling in centrifuge can be found in Madabhushi (2014).

The main dimensions and properties of the monopile model are shown in Table 2. The test setup can be seen in Fig. 6, with corresponding dimensions and dimensionless parameters in Table 3. For the tests performed, the recommendations of Klinkvort et al. (2018) were followed regarding the position of the monopile relative to the sides and bottom of the test box, as well as the dimensionless parameters associated with centrifuge modeling of monopiles in sandy soils. The tests were performed on the QZ and CA80 sands in the dry condition, which has been common practice in offshore monopile centrifuge studies (e.g., Futai et al., 2018).

For the compatibility of the various variables involved in the physical modeling, a gravitational acceleration factor of 96g was chosen. The relative stiffness (Kr) pile-soil values used in the tests were in the intermediate range between the rigid and flexible domains and close to the values of offshore wind towers installed in Europe (Abadie et al., 2019). The value of Kr is given through the equation established by Poulos (1982), which combines geometric and stiffness parameters of soil and pile materials.

Table 2. Model and prototype parameters

Parameter	Notation	Model	Prototype
External Diameter	D	19.16 mm	1.84 m
Internal Diameter	D_{int}	16.58 mm	1.59 m
Load Eccentricity	L_{ecc}	70.00 mm	6.72 m
Pile length (embedded)	L	96.15 mm	9.23 m
Wall thickness	t	1.29 mm	0.12 m
Stiffness	E_pI_p	0.20 KN.m²	17.42 GN.m²

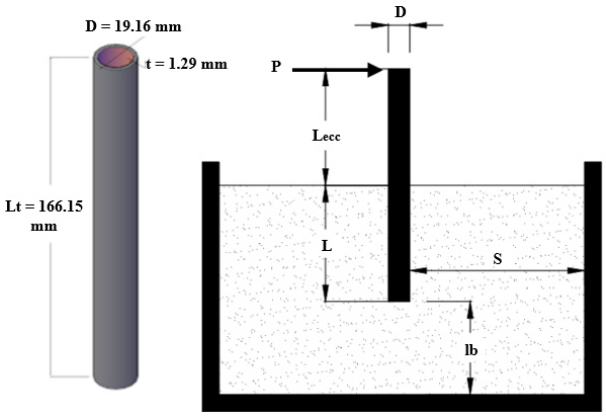

Figure 6. Monopile dimensions and test setup.

Although ideally the monopile installation should be performed in-flight (Dyson and Randolph, 2001), most studies presented in the literature use installation of the monopile in the natural gravitational field (1g) (e.g., Futai et al., 2018), as was also the case in the present study.

Table 3. Test setup dimensionless parameters

Parameter	Dimensionless parameter	Value
Pile diameter to grain size ratio	D/d_{50}	106.44
Monopile wall thickness ratio	t/D	0.07
Embedded pile length ratio	L/D	5.02
Lateral distance ratio	S/D	5.24
Bottom distance ratio	l_b/D	2.56
Scaled stiffness	EI_{prot}/N^4	0.205

The tests consisted of applying controlled lateral displacement through the actuator attached to the ball joint located near the top of the monopile, depicted in Fig. 7 (b), at a constant rate and measurement of the corresponding lateral load. The displacement at the load application point was measured by a magnetic sensor connected to the actuator (70 mm above the mudline), while near ground level (14.7 mm above the mudline) the measurement was performed using a laser sensor. The monopile was instrumented with five pairs of full-bridge strain gauges (Fig. 7 (a)) in order to obtain p-y curves for the monopile, but this topic is outside the scope of this paper.

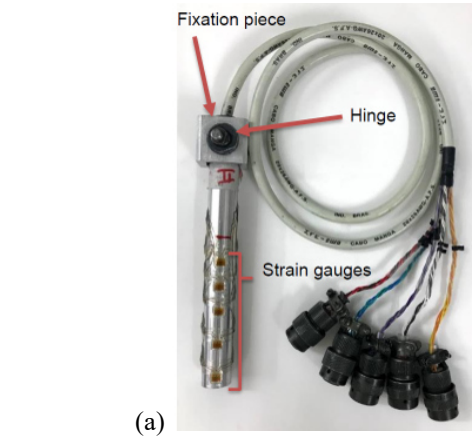

(a)

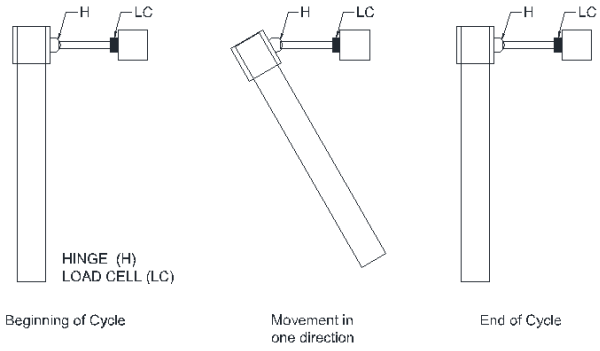

(b)

Figure 7. Monopile (a) photo with instrumentation; (b) loading and unloading diagram.

3.2. Benchmark monotonic tests

The monotonic tests presented in this section fall within the scope of a Benchmark exercise (Bienen et al, 2019) with the participation of other research institutions (CEIGR, COFS, DTU, IFSTTAR, KAIST, TUDelft e

UoN)[1], the aim of which was to compare results from geotechnical centrifuge modeling using different quartz sands, all at 80% relative density, simulating the same laterally loaded monopile prototype.

Two tests were performed with monotonic loading, M1 and M2, applying maximum displacement at ground level (y) of approximately 0.3 times the model diameter; the maximum displacement corresponding to the point of load application was 11 mm. Both tests were conducted at a commonly agreed displacement-controlled rate of 0.32 mm/s, measured at the point of application of the load eccentricity L_{ecc} (see Fig. 6).

Fig. 8 summarizes the test results in prototype scale as a function of displacement at ground level. The load-displacement curves (Fig. 8 (a)) of the two testes yielded essentially the same results, indicating good repeatability of the response. Fig. 8 (b) shows the results in terms of the normalized bending moment (M/Mr) versus normalized horizontal displacement (y/D). The moment M is derived from the product of the horizontal load (P) times the load eccentricity (L_{ecc}) and Mr is the value corresponding to the displacement of 0.1D, in this case, the ultimate limit state criterion adopted by Klinkvort, 2012. The test results were compared with the equation proposed by Abadie (2015), which shows stiffer initial behavior for theoretical values up to y/D ~ 0.04, but with essentially equal values for the ultimate state condition (y/D = 0.1).

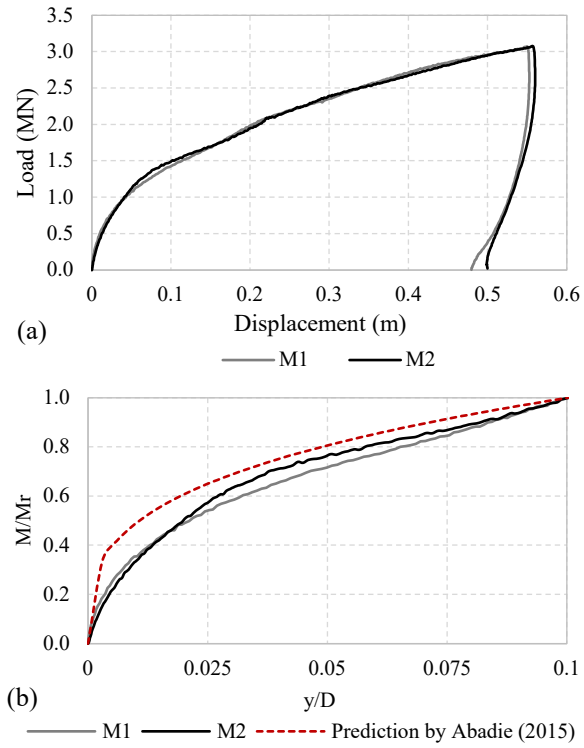

Figure 8. Monotonic loading: (a) load x displacement at prototype scale for two tests; (b) normalized moment x normalized displacement - experimental curves (solid lines) x theoretical (dashed line).

Lopes et al. (2022) developed a numerical model considering the modulus degradation shown in Fig. 5, which predicted quite well the results of tests M1 and M2, particularly at small displacement conditions.

Fig. 9 compares the lateral load versus mudline displacement results from the COPPE (M1 and M2) tests with the TU Delft tests performed with similar scale factors. The results are presented at prototype scale in Fig. 9 (a) and in a normalized plot in Fig. 9 (b). In this case the load P is normalized by $N\gamma_s D^3$, where N is the centrifuge scale factor, γ_s is the soil unit weight, and D is the monopile diameter. In the horizontal axis in Fig. 9 (b) the ground level displacement y, is normalized by the monopile external diameter.

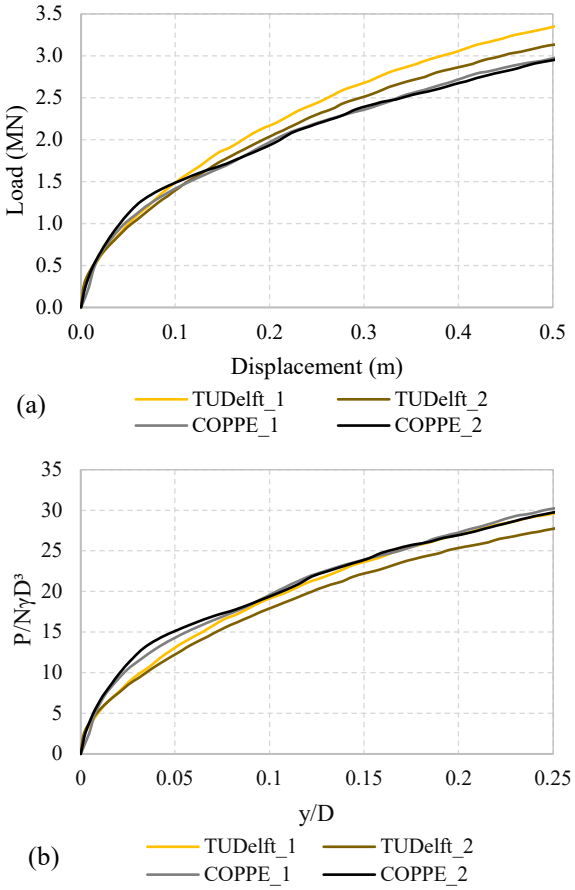

Figure 9. Experimental results COPPE and TU Delft – prototype scale (a) and normalized plot (b).

3.3. Monotonic and cyclic tests

After validation of the test procedure, as presented above, monotonic and cyclic tests were performed. The continuous sequence of side loading in the model was done in three steps: a) monotonic loading 1 (before cycling); b) cyclic loading with 4800 cycles; c) monotonic loading 2 (after cycling).

The parameters of the tests performed are presented in Table 4. In the monotonic loading step, displacement greater than 0.1D was applied at ground level, whose

[1] CEIGR: University of Sheffield; COFS: University of Western Australia; DTU: Technical University of Denmark; IFSTTAR: French Institute of Science and Technology for Transport, Development and Networks; KAIST: Korea Advanced Institute of Science and Technology; TU Delft: Delft University of Technology; UoN: University of Nottingham.

objective was to evaluate the variation of the ultimate lateral load as a function of the number of loading cycles, while for the cyclic step the main objective was to evaluate the variation of soil stiffness over the loading cycles. The cyclic tests were within the service limit state of offshore wind towers, whose criterion adopted was displacement equivalent to 0.5º rotation at the top of the monopile (Achmus et al., 2009). The cyclic action was quasi-static, seeking only to impose a degradation condition to the soil without, however, representing the actual frequency of loading in situ, which is usually below 0.1 Hz (LeBlanc, 2009).

Table 4. Main features of monotonic and cyclic tests

Test	Dr (%)	V(1) (mm/s)	Displacement (2) (mm)
C1-QZ	80	1.02	30 (monotonic)
C1-CA80	78		3.5 (cyclic)

(1) Controlled displacement rate at the point of load application (L_{ecc}).
(2) Displacement relative to the load application point (L_{ecc})

Fig. 10 presents, at prototype scale, an overview of the tests as a function of applied lateral load versus ground level displacement for all test phases. Fig. 10 (a) shows the results for C1-QZ, while Fig. 10 (b) shows the results for C1-CA80. When comparing the monotonic loading curves before and after cyclic loading in these graphs, an increase in the tangent stiffness of the soil can be seen, either for the QZ or CA80 sand. This behavior can be explained by the densification effect of the soil, as observed by other authors (e.g., Klinkvort, 2012; Kirkwood, 2015).

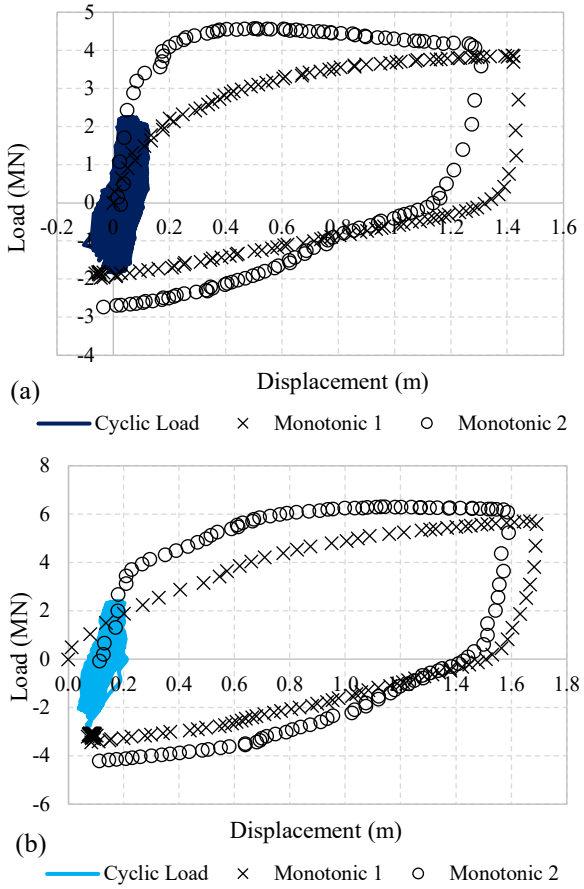

Figure 10. Load-displacement (a) C1-QZ (b) C1-CA80.

The variation in the lateral load capacity (assumed here at y = 0.1D) due to the soil cycling process can be seen in Fig. 11 and Table 5. For the adopted criterion (dashed line in Fig. 11), the different sands yielded almost equal values (2.0 and 1.9 MN before cycling and 4.0 and 4.1 MN after cycling for the QZ and CA80 sands, respectively).

Although the CA80 sand has a greater peak friction angle, no significant differences were observed in terms of load capacity for the adopted criteria (y = 0.1D). However, if a wider range of displacement is considered, especially for y > 0.4 D, a greater lateral load capacity is evident for the CA80 sand, apparently due to its higher friction angle. Particle grain breakage resulting in interlock between adjacent soil particles associated at larger displacements, is another factor that may have influenced the increase in load capacity of the CA80 sand.

The gains in load capacity, as a function of the cyclic loading process, were relatively close for both materials, with a gain of 100% for the QZ sand and 116% for the CA80 sand. These gains may be related to the soil densification phenomenon and, in the case of the CA80 sand, also from the occasional grain breakage process.

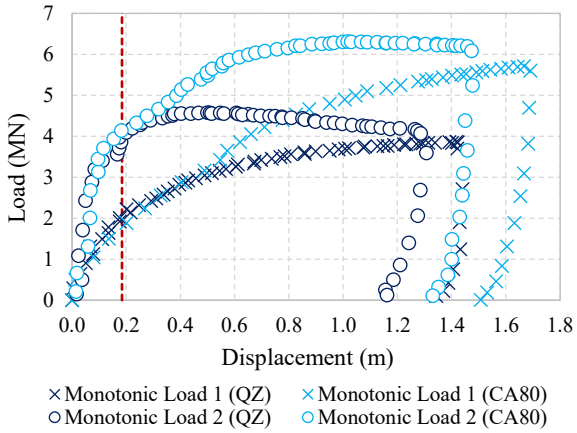

Figure 11. Monotonic loading before and after soil cycling.

Table 5. Ultimate load for monotonic tests before and after cycles

	Ultimate load (y = 0.1D)	
Sand	**Before cycles**	**After cycles**
QZ	2.0 MN	4.0 MN
CA80	1.9 MN	4.1 MN

Fig. 12 shows the data from the tests as a function of time. For both cases, a higher peak load is evident after cycling compared to the first monotonic load, as reported above. Moreover, the mobilized load increases exponentially in the first cycles, followed by an approximately linear increase until stabilization in the last third of the 4800 cycles applied. In Fig. 12 (c) emphasis is given to some loading cycles (1st, 10th, 25th, 50th, 100th, 250th, 500th, 1000th, 2000th and 4800th), where the effect of soil cycling on the mobilized lateral load can be clearly observed. In the first cycles there is a more noticeable difference in the mobilized load between QZ and CA80, but the values are close in the last cycles. Regarding the mobilized peak load (dashed lines), both shape and magnitude are essentially the same for QZ and CA80.

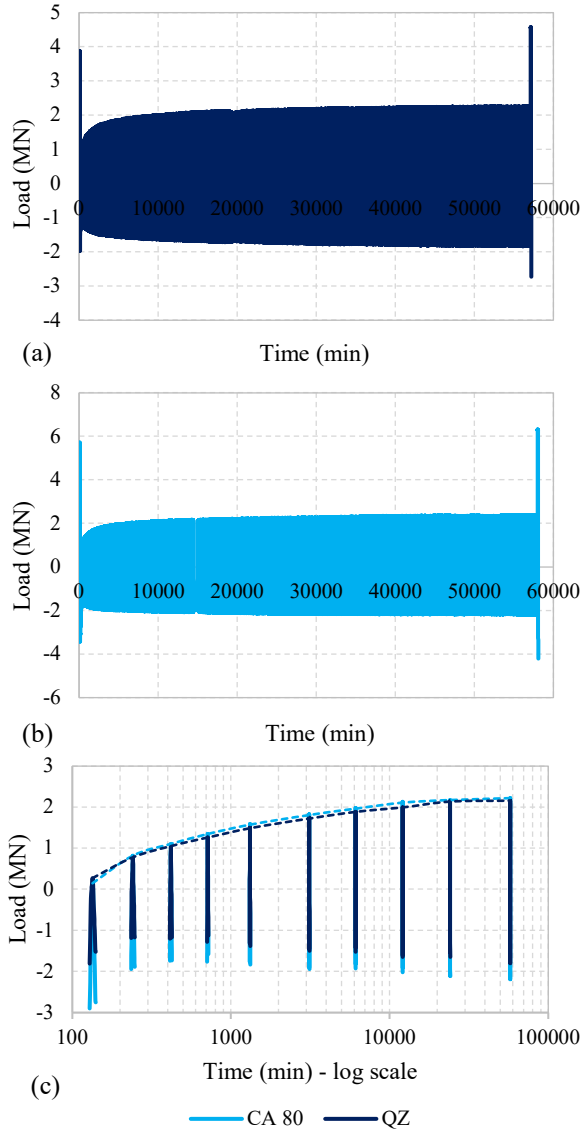

Figure 12. Load-time curves - C1-QZ (a, c) and C1-CA80 (b, c) tests.

Fig. 13 shows the definition of the secant stiffness (Fig. 13 (a)) and its variation with the number of load cycles (Fig. 13 (b)). Initially, the CA80 sand and the QZ sand present similar values of secant stiffness. However, with the increasing number of cycles the secant stiffness of the QZ sand becomes larger. The lower secant stiffness of the carbonate sand is related to its smaller shear modulus (for shear strains greater than 0.001%) in comparison with the quartz sand, as shown in Fig. 5.

4. Conclusions

The main conclusions concerning the mechanical behavior of the quartz and carbonate sands are:

- The result for the QZ sand shows little difference in the G_{max} values at loading and unloading. However, for the CA80 sand, the values of G_{max} at unloading are higher than at loading.
- Shear modulus degradation and damping ratios for the CA80 sand is higher than for the QZ sand, especially for shear strains greater than 0.001%.

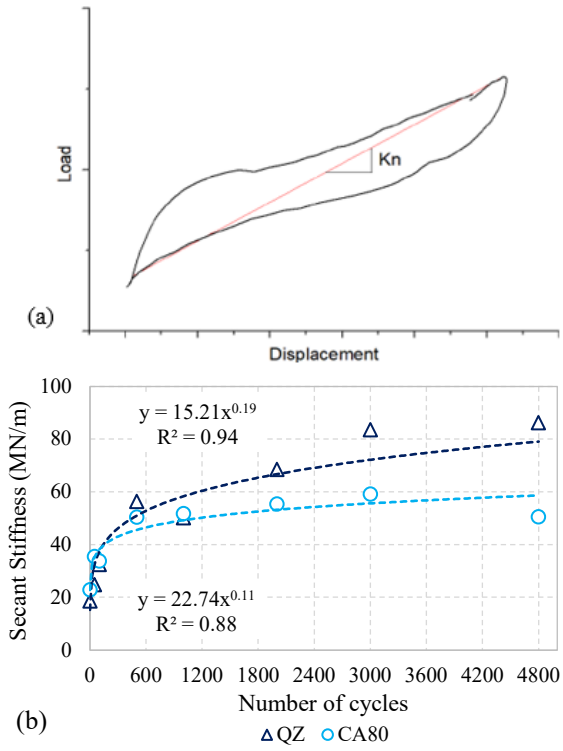

Figure 13. Secant stiffness K_n: (a) Definition; (b) K_n versus the number of cycles.

The following conclusions can be drawn from the geotechnical centrifuge tests:

- The QZ and CA80 sands yielded similar lateral load capacity values at each monotonic loading stage for an ultimate load criterion of 0.1D.
- For displacements up to 0.1D there was no evident influence of the larger peak friction angle of the CA80 sand on the ultimate load capacity, however, for y > 0.4 D, a greater mobilized load is evident for this soil due to its higher peak friction angle.
- The gain in load capacity due to soil cycling was consistent for both materials, with 100% gain for the QZ sand and 116% for the CA80 sand.
- The CA80 sand presents slightly higher stiffness in the first cycles of loading. However, with an increase in the number of cycles the secant stiffness of the QZ sand has a more significant increase and becomes larger, especially after 500 cycles.

Finally, it may be concluded that monopile foundations installed in both dense quartz sand and in dense carbonate sand may withstand cyclic lateral loading with satisfactory behavior in terms of serviceability as well as ultimate limit state conditions. It should be pointed out, however, that the present study has some limitations as real monopile foundations are subjected to around 10^7 cycles in their lifetime and the number of cycles simulated in the present study is smaller.

Acknowledgements

The authors would like to thank the support of the funding agencies Brazilian National Council for Scientific and Technological Development (CNPq), the

Rio de Janeiro and São Paulo Research Foundations, FAPERJ and FAPESP. Thanks are also due to Dr. Samuel Tarazona for the technical support in the centrifuge tests and to Dr. Cristian Soriano for reviewing the paper.

References

Abadie, C. N. 2015. "Cyclic lateral loading of monopile foundations in cohesionless soils", PhD Thesis, University of Oxford.

Abadie, C. N., Byrne, B. W., Houlsby, G. T. 2019. "Rigid pile response to cyclic lateral loading: Laboratory tests", Geotechnique, v. 69 (10), pp. 863–876. https://doi.org/10.1680/jgeot.16.P.325

Achmus, M., Kuo, Y-S., Abdel-Rahman, K. 2009. "Behavior of monopile foundations under cyclic lateral load", Computer and Geotechnics, v. 36 (5), 725-735. https://doi.org/10.1016/j.compgeo.2008.12.003

Almeida, M. S. S., Oliveira, W. L., Medeiros, C. J., Porto, E. C. 1987. "Laboratory tests and design parameters for offshore piles in Campos Basin calcareous sands", 6th International on Offshore Engineering, pp. 215-225.

Almeida, M. S. S., Almeida, M. C. F., Trejo, P. C., et al. 2014. "The geotechnical beam centrifuge at COPPE centrifuge laboratory", 8th international Conference of Physical Modelling in Geotechnics.

ASTM 4254. 2016. "Standard test methods for minimum index density and unit weight of soils and calculation of relative density", American Society for Testing and Materials, USA. https://doi.org/10.1520/D4254-16

ASTM D4015. 2017. "Standard test methods for modulus and damping of soils by fixed-base resonant column devices", American Society for Testing and Materials, USA. https://doi.org/10.1520/D4015-15

Bienen, B., Klinkvort, R. T., Fan, S., Black, J., Bayton, S., Thorel, L., Madabhushi, G. S. P., Askarinejad, A., Li, Q., et al. 2019. "Centrifuge benchmark testing of laterally loaded monopiles in sand", 16th Asian Regional Conference on Soil Mechanics and Geotechnical Engineering. http://resolver.tudelft.nl/uuid:f80f5f93-fbe0-4ddc-95c9-94583f4d1526

Blaker, Ø., Lunne, T., Vestgården, T., Krogh, L., Thomsen, N. V., Powell, J. J. M., Wallace, C. F. 2015. "Method dependency for determining maximum and minimum dry unit weights of sands", 3rd International Symposium on Frontiers in Offshore Geotechnics, v. 3, pp. 1159-1166. https://doi.org/10.1201/b18442-174

Buckley, R. M, et al. 2020. "Large diameter pile testing for offshore wind applications with a focus on cyclic lateral loading and rate effects", 4th International Symposium on Frontiers in Offshore Geotechnics, pp. 1403–1412.

Byrne, B.W., et al. 2020. "Cyclic laterally loaded medium scale field pile testing for the Pisa project", 4th International Symposium on Frontiers in Offshore Geotechnics, pp. 1323–1332. http://resolver.tudelft.nl/uuid:a24d76c2-c3aa-4768-aacc-bc8984d9a3cd

Correia, A. G., Barros, J. M., Santos, J. A., Sussumu, N. 2001. "An approach to predict shear modulus of soils in the range of 10^{-6} to 10^{-2} strain levels", IV International Conference on Recent Advances in Geotechnical Earthquake Engineering and Soil Dynamics.

Drnevich, V. P., Werden, S., Ashlock, J. C., Hall, J. R. J. 2015. "Applications of the new approach to resonant column testing", Geotechnical Testing Journal, v. 38 (1), pp. 23–39. https://doi.org/10.1520/GTJ20140222. ISSN 0149-6115

Dyson, G. J., Randolph, M. F. 2001. "Monotonic lateral loading of piles in calcareous sand", Journal of Geotechnical and Geoenvironmental Engineering, v. 127 (4), pp. 346–352. https://doi.org/10.1061/(ASCE)1090-0241(2001)127:4(346)

El-Reedy, M. A. 2012. "Offshore structures: design, construction and maintenance", 1st Edition, Gulf Professional Publishing, Oxford, UK, pp. 208-253.

EPBR "Offshore wind farms under licensing in Brazil reaches 80 GW", Available at: https://epbr.com.br/eolicas-offshore-em-licenciamento-no-brasil-somam-80-gw-de-potencia/ , accessed on: 05/06/2022 [in Portuguese].

Flores Lopez, F. A., Taboada, V. M., Gonzalez Ramirez, Z. X., Cruz Roque, D., Barrera Nabor, P., & Dantal, V. S. 2018. "Normalized modulus reduction and damping ratio curves for bay of Campeche carbonate sand", Offshore Technology Conference. https://doi.org/10.4043/29010-ms

Futai, M. M., Dong, J., Haigh, S. K., et al. 2018. "Dynamic response of monopiles in sand using centrifuge modelling", Soil Dynamics and Earthquake Engineering, v. 115, pp. 90–103. https://doi.org/10.1016/j.soildyn.2018.08.007

Garske, R. B. 2020. "Personal communication".

Kirkwood, P. B. 2015. "Cyclic lateral loading of monopile foundations in sand", DSc Thesis, University of Cambridge.

Klinkvort, R. T. 2012. "Centrifuge modelling of drained lateral pile-soil response", PhD Thesis, Technical University of Denmark.

Klinkvort, R. T., Black, J. A., Bayton, S. M., et al. 2018. "A review of modelling effects in centrifuge monopile testing in sand", Physical Modelling in Geotechnics, v. 1, pp. 719–724. https://doi.org/10.1201/9780429438660-108

Leblanc, C. B. 2009. "Design of Offshore Wind Turbine Support Structures: Selected topics in the field of geotechnical engineering", PhD Thesis, Aalborg University.

Lopes, G. K., Sousa, J. R. M., Almeida, M. C. F., Almeida, M. S. S. 2023. "A numerical methodology to predict the lateral load response of monopiles installed in sand considering soil stiffness degradation", Ocean Engineering, v. 270. https://doi.org/10.1016/j.oceaneng.2023.113723

Madabhushi, G. 2014. "Centrifuge modelling for civil engineers", 1st Edition, Taylor & Francis Group, USA.

Menq, F. 2003. "Dynamic properties of sandy and gravelly soils", Phd Thesis, University of Texas.

Miura, S., Toki, S. 1982. "A Sample preparation method and its effect on static and cyclic deformation-strength properties of sand", Soils and Foundations, v. 22 (1), pp. 61-77. https://doi.org/10.3208/sandf1972.22.61

OECO "The unknown 'rolling stones' reefs", Available at: https://oeco.org.br/analises/rodolitos-os-desconhecidos-recifes-rolling-stones/ on: 06/06/2022 [in Portuguese].

OWM "Offshore Wind Market Report: 2021 Edition", Available at (accessed on 06/06/2022): https://www.energy.gov/eere/wind/articles/offshore-wind-market-report-2021-edition-released Poulos, H. G. 1982. "Single pile response to cyclic lateral load", Journal of Geotechnical and Geoenvironmental Engineering, v. 108 (3), pp 355–375. https://doi.org/10.1061/AJGEB6.0001255

Poulos, H. G., Uesugi, M., Young, G. S. 1982. "Strength and deformation properties of Bass Strait carbonate sands", Geotechnical Engineering, v. 13 (2), pp. 189-211.

Senetakis, K., Madhusudhan, B. N. 2015. "Dynamics of potential fill–backfill material at very small strains", Soils and Foundations, v. 55 (5), pp. 1196–1210. https://doi.org/10.1016/j.sandf.2015.09.019

Watson, P., Bransby, M. F., Delimi, Z., et al. 2019. "Foundation design in offshore carbonate sediments–building on knowledge to address future challenges", XVI Pan-American Conference on Soil Mechanics and Geotechnical Engineering, pp. 240-274. https://doi.org/10.3233/ASMGE190022